Human Molecular Genetics, 2005, Vol. 14, No. 13 ***1825–1837***
doi:10.1093/hmg/ddi189
Advance Access published on May 25, 2005

Treatment with trkC agonist antibodies delays disease progression in neuromuscular degeneration (*nmd*) mice

Rocio Ruiz[1], John Lin[2], Alison Forgie[2], Davide Foletti[2], David Shelton[2], Arnon Rosenthal[2] and Lucia Tabares[1,*]

[1]Department of Physiology and Biophysics, School of Medicine, University of Seville, Seville, Spain and [2]Rinat Neuroscience Corporation, 3155 Porter Drive, Palo Alto, CA 94304, USA

Received January 17, 2005; Revised and Accepted May 4, 2005

Spinal muscular atrophy with respiratory distress type 1 (SMARD1) is a fatal autosomal recessive disorder seen in infants. It is characterized by lower motor neuron degeneration, progressive muscle paralysis and respiratory failure, for which no effective treatment exists. The phenotype of neuromuscular degeneration (*nmd*) mice closely resembles the human SMARD1. The identification of the mutated mouse gene in *nmd* mice, *Ighmbp2*, led to the discovery of mutations of the homologous gene in humans with SMARD1. We have studied the *nmd* mouse model with *in vivo* electrophysiological techniques and evaluated the efficacy of Mab2256, a monoclonal antibody with agonist effect on the tyrosine kinase receptor C, trkC, on disease progression in *nmd* mice. Treatment with Mab2256 resulted in a significant but transient improvement of muscle strength in *nmd* mice, as well as normalization of the neuromuscular depression during high-frequency nerve stimulation. These results suggest the potential of using monoclonal agonist antibodies for neurotrophin receptors in lower motor neuron diseases such as SMARD1.

INTRODUCTION

Spinal muscular atrophy with respiratory distress type 1 (SMARD1) is a clinical variant of spinal muscular atrophy (SMA), the second most common autosomal recessive disorder and the most common genetic cause of death in childhood. SMA and SMARD1 are characterized by degeneration of lower motor neurons associated with progressive muscle paralysis. The majority of SMA cases is caused by mutations in the survival motor neuron gene (*SMN*) (1), whereas SMARD1 is caused by mutations in a different gene, the immunoglobulin μ-binding protein 2 gene (*IGHMBP2*) (2–5). SMARD1 patients suffer from early impairment of the respiratory function due to diaphragmatic involvement (4). Currently, there is no effective therapy for either SMARD1 or SMA in general (6), despite some pilot clinical trials with positive results (7).

The neuromuscular degeneration (*nmd*) mice harbour a spontaneous mutation in the mouse *Ighmbp2* gene, a member of a DNA/RNA helicase/ATPase protein family (8–10). The genetic defect consists of a single mutation (A–G) in intron 4, resulting in 80% abnormally spliced and 20% full-length transcript (9). The *nmd* mice display a disease phenotype similar to the milder form of human SMARD1, as the functional IGHMBP2 expression is not completely abolished in the *nmd* mice (9). Muscular weakness starts to develop after the second week of birth, progressing to severe neurogenic muscle atrophy of the extremities (8–11).

Neurotrophic factors have been considered as potential therapeutics for motor neuron diseases. This expectation has been based on the survival-promoting properties of these molecules in animal embryonic motor neurons in culture, their positive biological effects on nerves after axotomy and on alleviating the pathological symptoms in animal models of neurodegenerative diseases (12–15). Given the promising results obtained in most of the *in vitro* and *in vivo* studies, exogenous neurotrophins have been used in clinical trials for patients with Alzheimer's disease, amyotrophic lateral sclerosis, peripheral neuropathies, Parkinson's disease and Hungtinton's disease.

One practical difficulty in applying neurotrophins is that all these proteins have a relatively short half-life, whereas the neurodegenerative diseases are chronic and require

*To whom correspondence should be addressed. Tel: +34 954556574; Fax: +34 954551769; Email: ltabares@us.es

long-term treatment. Therapeutic agonist antibodies targeting the neurotrophin receptors may represent a novel approach for neurodegenerative diseases due to their high specificity and long half-life.

In the present study, we perform an *in vivo* electrophysiological characterization of hind limb and diaphragm muscles of the *nmd* mouse model of SMARD1 and we evaluate the potential efficacy of an agonistic monoclonal antibody (Mab2256) for tyrosine kinase receptor C (trkC) in this mouse model. We show that Mab2256 treatment prevented the initial decline of muscular strength and it led to the electrophysiological improvement of muscular function, consisting of restoration to normality of the level of depression during repetitive electrical stimulation. However, such initial improvements did not translate into muscle fibre preservation or survival benefit, highlighting the areas for further optimization of this therapeutic strategy.

RESULTS

Agonistic and pharmacokinetic properties of the trkC antibody Mab2256

Monoclonal antibodies against the human trkC extracellular domain were generated and screened for agonist activity using a cell-based receptor tyrosine phosphorylation assay (16). One monoclonal antibody, Mab2256, of the murine IgG_1 isotype was found to be a specific binder of trkC receptor without cross reactivity with trkA or trkB (data not shown). In the stable trkC expressing CHO cells, Mab2256 induces trkC tyrosine phosphorylation with the half-maximum effective concentration (EC_{50}) of 0.87 nM, whereas NT-3 does so with EC_{50} of 1.09 nM (Fig. 1A). Consistent with its ability to activate trkC receptor, Mab2256 also supports the survival of the embryonic rat trigeminal neuron cultures in a dose-dependent fashion with an EC_{50} of 2.58 nM, whereas NT-3 has an EC_{50} of 0.73 pM (Fig. 1B).

Next, we investigated the pharmacokinetic property of Mab2256. We found the elimination phase half-life ($t_{1/2}$) of Mab2256 from serum to be $\sim$199 h when given intraperitoneally in mice. This is the long circulating half-life expected of an antibody, and it compares favourably with the published plasma half-life of the endogenous trkC agonist, NT-3, at around 1.28 min (17).

Effect of Mab2256 on motor performance and survival in *nmd* mice

Mutant mice appeared indistinguishable from wild-type at birth but they fed and grew poorly after 2 weeks of birth. Hence, the homozygous mutants were easily identifiable from wild-type and heterozygous littermates by their lower body weight (Fig. 2A). In addition, mutant mice exhibited progressive loss of muscle mass and a marked decrease in fore- and hind-limb grip strength (8–11). They could not support their body against gravity, were unable to grasp a cage cover and gradually lost muscle mass of the shoulder and pelvic girdles.

We examined whether treatment with Mab2256 (5 mg/kg body weight, two times per week, starting on postnatal day 20, i.e. P20) could prevent the progressive loss of muscular function that occurs in *nmd* mice. The presence of the monoclonal antibody in serum was confirmed by ELISA analysis in mice injected with Mab2256 ($n = 10$) or phosphate buffered saline (PBS) ($n = 5$) for 6–8.5 weeks. The mean concentration of the Mab2256 antibody in serum was 10.6 ± 3.4 μg/ml ($n = 10$ of Mab2256 injected mice). No side effects were observed in wild-type and *nmd* Mab2256-treated mice. There was no significant differences in body weight between treated and untreated mice (Fig. 2A and B): on P60, the body weight of Mab2256-treated mutants was 14.5 ± 0.2 g ($n = 16$) and that of untreated or vehicle control was 14.2 ± 0.83 g ($n = 8$).

Standard neurological examinations were performed in untreated and Mab2256-treated mice from 4–10 weeks of age. To explore fore limb-gripping strength, mice were suspended upon a metal wire 10 cm above the floor by their fore limbs. The duration that the mouse remained suspended was recorded. Untreated *nmd* mice (PBS-injected $n = 5$; not injected $n = 9$) showed a nearly complete loss of grip strength in their fore limbs throughout the entire study (Fig. 2C, filled squares). Strikingly, the Mab2256-treated *nmd* mice retained the grip strength for several weeks (Fig. 2C, triangles). The mean duration that PBS-injected *nmd* mice were able to maintain themselves on the wire was 0.8 ± 0.6 s at 4 weeks of age ($n = 5$), whereas at the same age in Mab2256-treated *nmd* mice, it was 5.1 ± 1.6 s (nine mice, six litters) ($P < 0.03$), and 4.9 ± 1.4 s a week later ($P < 0.034$). Heterozygous performance (Fig. 2C, grey squares; $n = 8$) was identical to that of wild-type siblings (Fig. 2C, white squares).

Motor coordination was also measured by the ability of the *nmd* mice to maintain themselves on a constant speed rotating rod (test time duration: 10 s). Untreated *nmd* mice showed very poor balance in comparison with wild-type and heterozygous littermates (Fig. 2D and E), ($P < 0.001$), whereas Mab2256-treated *nmd* mice showed significantly better motor coordination 1 week after treatment (Fig. 2D and F), ($P < 0.018$). These results indicated that Mab2256 treatment ameliorated disease progression in *nmd* mice.

To answer whether Mab2256 affected survival, life spans of untreated and Mab2256-treated *nmd* mice were recorded from weaning to adulthood. No significant increase in life span was observed (Mann–Whitney rank-sum test): the median life span of Mab2256-treated mutant mice was 69 days ($n = 15$), whereas that of untreated *nmd* mice was 62 days ($n = 30$) (Fig. 2G).

Electrical neuromuscular activity in *nmd* mice

In vivo electromyography (EMG) measurements were performed on P70 in the medial gastrocnemius (MG). We first stimulated the sciatic nerve by a single current pulse of supramaximal amplitude and recorded the compound muscular action potential (CMAP). The mean amplitude of the CMAP in the *nmd* mouse was reduced to $<50\%$ of the control value (Fig. 3A; 22.9 ± 5.6 mV, $n = 9$ and 48.8 ± 4.8 mV, $n = 14$, respectively; $P < 0.002$). The administration of Mab2256 had no significant effect on the mean amplitude of the CMAP in *nmd* (24 ± 3.1 mV, $n = 7$) or wild-type mice on P70 (61 ± 9.2 mV, $n = 8$) (Fig. 3A), suggesting that the

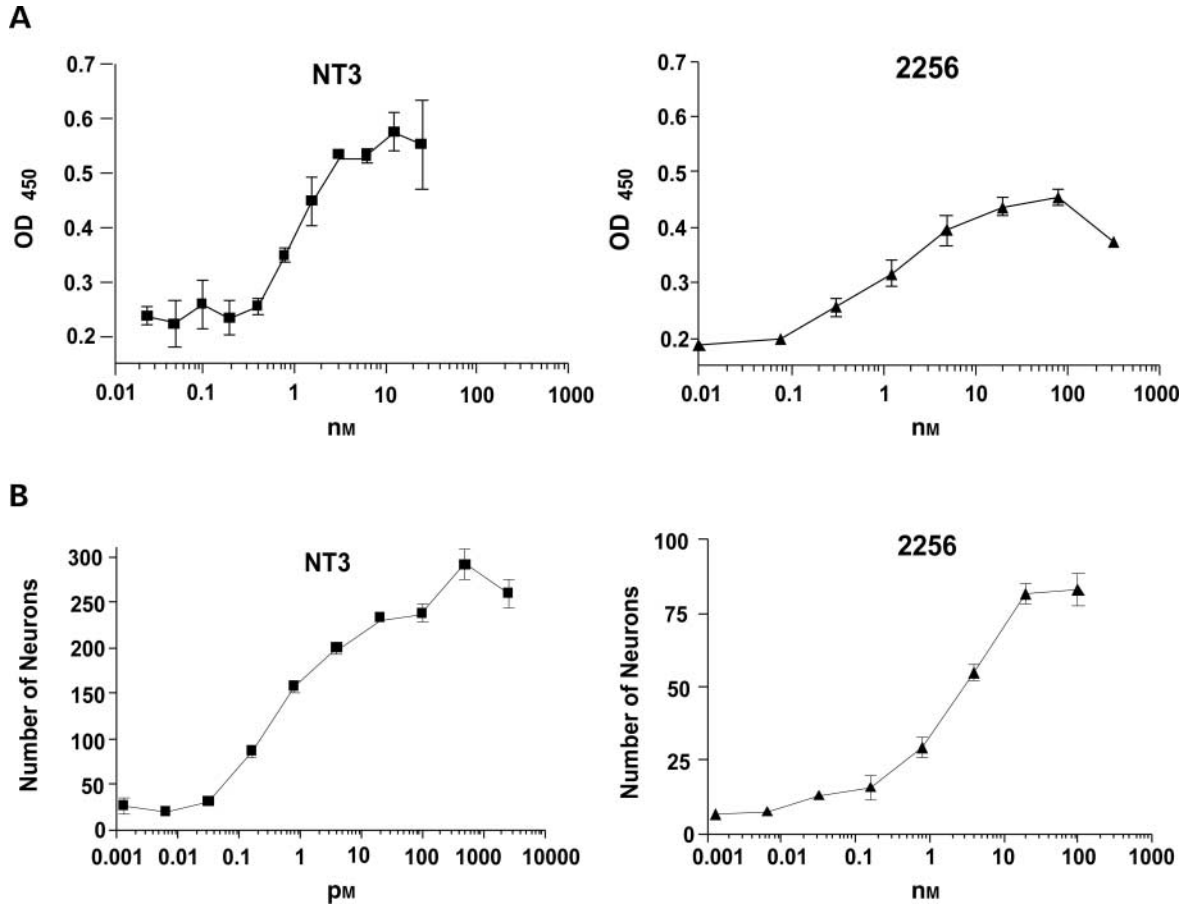

Figure 1. Monoclonal antibody Mab2256 can activate the trkC receptor and support trigeminal neuronal survival in culture. (**A**) Increasing and saturable levels of trkC receptor phosphoryaltion (expressed in OD 450, the *y*-axis) were induced either by increasing concentrations of NT-3 (left panel), the endogenous trkC ligand, or by monoclonal antibody Mab2256 (right panel), a trkC antibody. (**B**) Increasing and saturable numbers of embryonic rat trigeminal neurons surviving 48 h in culture were supported by the presence of various concentrations of NT-3 (left panel) or Mab2256 (right panel) in the culture medium.

treatment protocol with Mab2256 was not able to stop the loss of motor fibres. To ask whether a trkB agonist may be better than a trkC agonist, we also treated a group of mutant mice with the trkB agonist NT-4/5 (5 mg/kg body weight, two times per week, starting at P20). In this case, the mean amplitude of the CMAP was not altered by NT-4/5 treatment, either (26.7 ± 7.1 mV, $n = 3$ on P70).

Mab2256 and NT-4/5 restore normal levels of high frequency-induced neuromuscular depression

To further investigate the neuromuscular electrical properties in *nmd* mice and the effect of Mab2256 and NT-4/5, we used paired pulses, and short-train stimuli at different frequencies, and studied the electromyographic responses. In the MG, the amplitudes of the CMAP responses (A1 and A2) to paired-pulse supramaximal stimuli (10 ms interval) in the *nmd* mice were much different from those in the wild-type. In wild-type mice, the amplitude of the second CMAP (A2) was slightly greater than or equal to the first response (A1) (Fig. 3B). In mutant mice, the amplitude of the second response was $21.4 \pm 0.03\%$ smaller than that of the first response ($n = 7$) (Fig. 3C) ($P < 0.005$). The areas under the CMAP curves changed accordingly with their amplitudes, indicating a real change in the number of fibres activated and not a pseudodepression (data not shown).

With 250 ms trains of stimuli at 100 Hz, the amplitude of the CMAPs in untreated wild-type MG showed a consistent pattern; they increased gradually during the first three to four stimuli, and then progressively decreased over the stimulation period until reaching a quasi-steady-state value of depression (Fig. 3D, upper trace; Fig. 3E, open squares). This pattern was very different from the one seen in untreated *nmd* mice that was characterized by a maximal drop in amplitude between the first and the second CMAP of the train, followed by a further decline over the recording period (Fig. 3D, second trace; Fig. 3E, filled squares). In untreated mutants, the depression was fast and the normalized amplitude of the CMAP at the end of the train was much less than in the wild-type ($55 \pm 6.9\%$, $n = 6$ and $82.5 \pm 7.4\%$, $n = 6$, respectively) ($P < 0.02$), suggesting an increase in the number of fibres where transmission had fallen below threshold for action potential generation. Repetition of the same pattern of stimuli after an interval of no stimulation (2–4 min) gave a nearly identical pattern of responses to each presentation of the stimuli train.

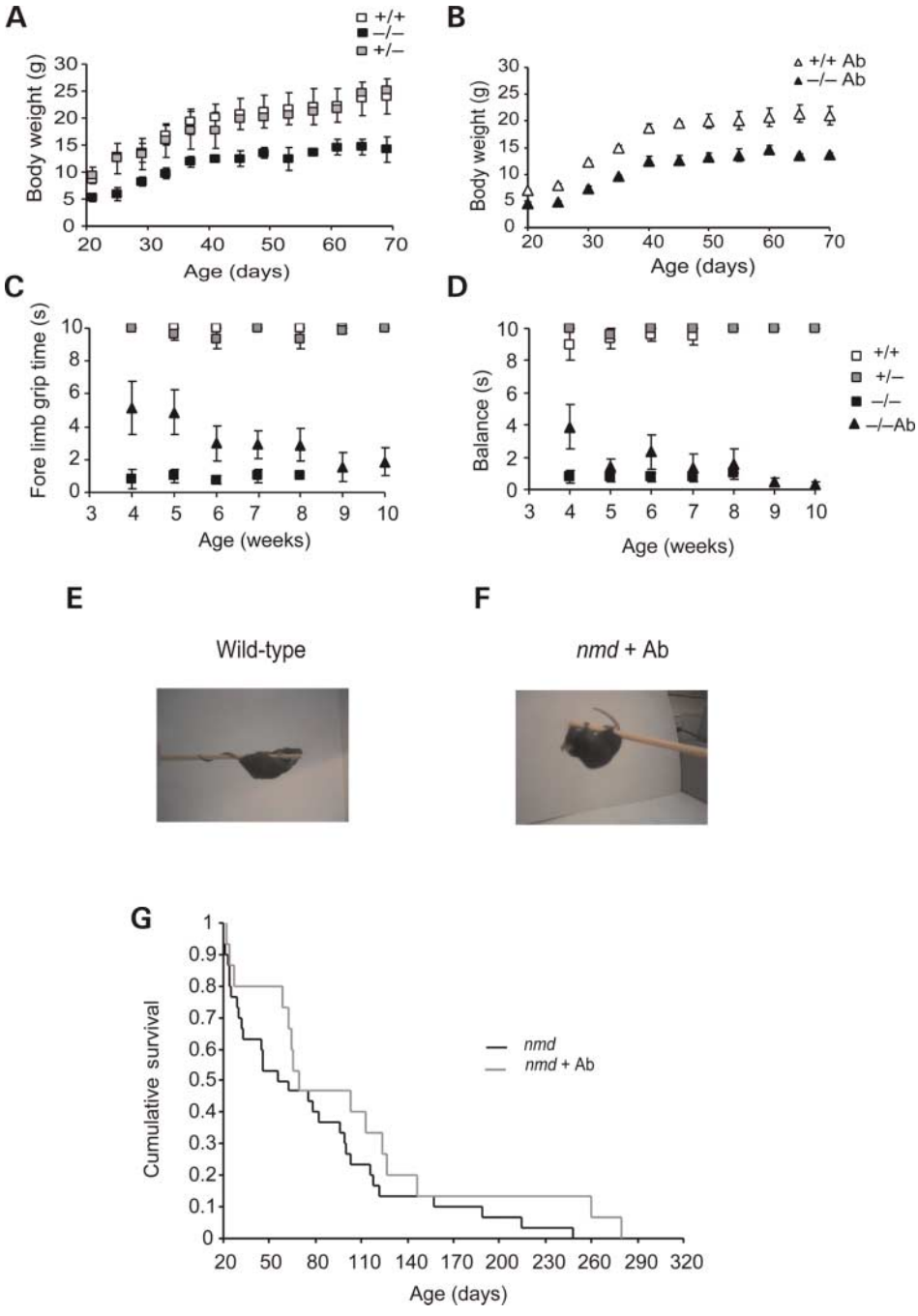

Figure 2. Disease signs and life span in *nmd* mice. (**A**) Mean body weight of wild-type (+/+) ($n = 8$), *nmd* (−/−) ($n = 8$) and heterozygous (+/−) ($n = 8$) mice from P20 to P70. (**B**) Mean body weight of wild-type (+/+ Ab) ($n = 10$) and *nmd* mice (−/− Ab) ($n = 16$) injected intraperitoneally with monoclonal antibody Mab2256, from week 3 to 11. (**C** and **D**) Fore limb grip time (C) and balance on the rod (D) of wild-type (+/+, open symbols) ($n = 14$), heterozygous (+/−, grey symbols) ($n = 8$), *nmd* injected with PBS (−/−, filled squares) ($n = 5$) and *nmd* mice injected with Mab2256 (−/− Ab, triangles) ($n = 9$). (**E** and **F**) Wild-type and Mab2256-treated mutant on the rod. The mutant was not able to use its tail to grasp the rod; nevertheless the mouse was able to maintain itself on the rotating rod for several seconds. Mab2256-untreated *nmd* mice were not able to maintain themselves for more than 1 s on the rod (data snot shown). (**G**) Kaplan–Meier survival analysis of untreated (*nmd*) ($n = 30$) and Mab2256-treated *nmd* (*nmd* Ab) ($n = 15$) mice. No significant differences for the two groups were obtained with the Mann–Whitney rank-sum test.

To assess the efficacy of Mab2256 on neuromuscular function, we recorded animals treated with the monoclonal antibody and compared the results with untreated mice. With repetitive nerve stimulation (100 Hz), the normalized amplitude of the CMAP at the quasi-steady-state was significantly larger in Mab2256-treated *nmd* mice ($74 \pm 4.1\%$, $n = 6$) (Fig. 3D, third trace) than in PBS-injected mutants ($55 \pm 6.9\%$, $n = 6$) (Fig. 3E, upper graph) ($P < 0.05$).

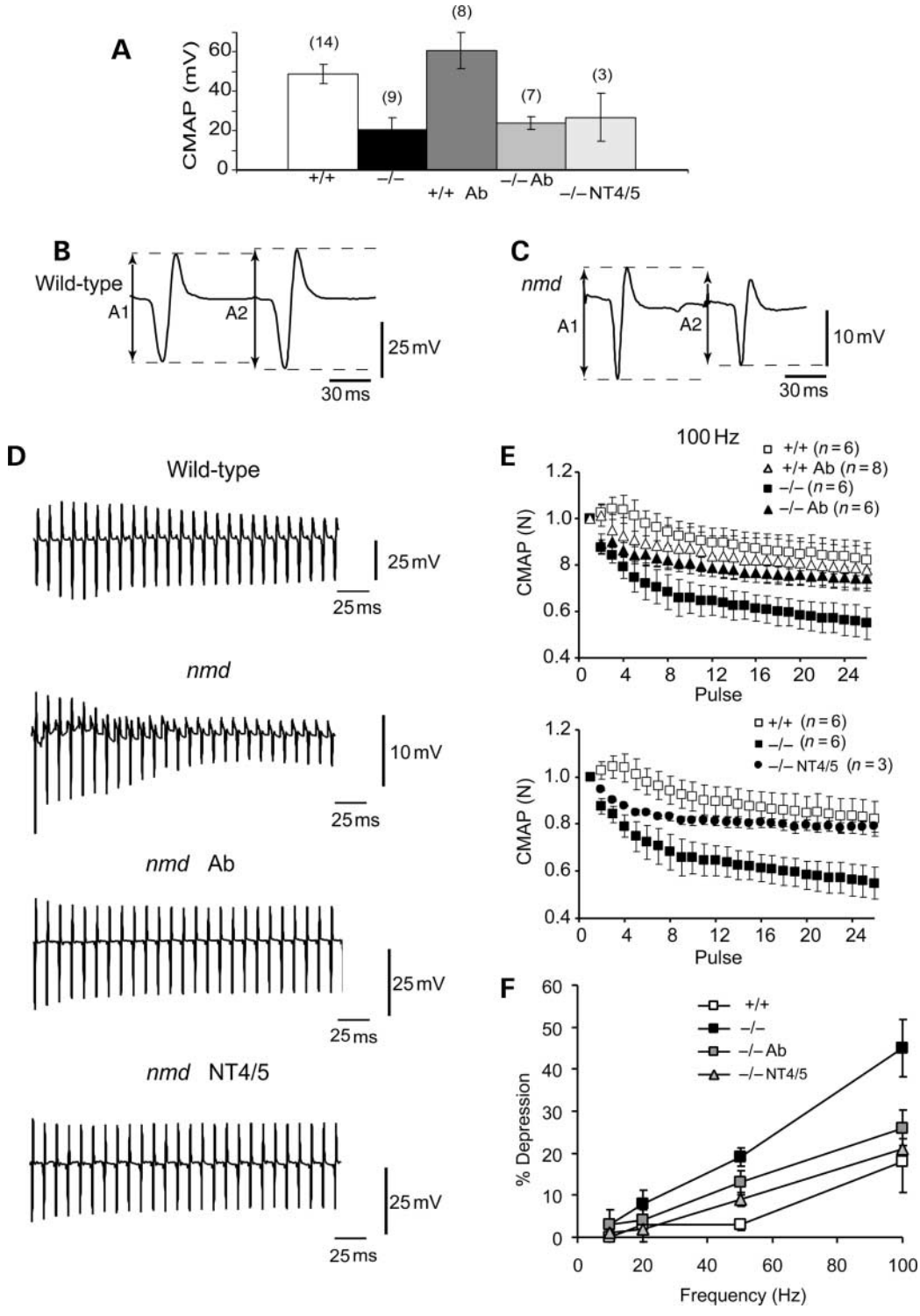

Figure 3. EMG measurements of CMAP amplitudes in the MG of wild-type and *nmd* mice reveal reduction of neurotransmission efficacy in the *nmd* mice. (**A**) Absolute amplitudes of CMAP (mean ± SEM) in response to supramaximal stimulation in untreated wild-type (+/+) ($n = 14$), *nmd* injected or not with PBS (−/−) ($n = 9$), wild-type treated with Mab2256 (+/+ Ab) ($n = 8$), *nmd* treated with Mab2256 (−/− Ab) ($n = 7$) and *nmd* mice treated with NT-4/5 (−/− NT4/5) ($n = 3$). (**B** and **C**) Representative responses of the CMAPs to a pair-pulse protocol in a wild-type (B) and in an *nmd* mouse (C). Interstimulus interval: 10 ms. The peak-to-peak amplitudes of the successive CMAPs (A1 and A2) are signalled by arrows. (**D**) Representative recordings during a train of stimuli at 100 Hz in a wild-type (upper trace) and three *nmd* mice: untreated (second trace), treated with Mab2256 (third trace) and treated with NT-4/5 (fourth trace). (**E**) Depression of CMAP amplitudes (normalized to the first response) during a train of stimuli of 250 ms at 100 Hz in untreated wild-type mice (+/+) ($n = 6$), Mab2256-treated wild-type (+/+ Ab) ($n = 8$), PBS injected *nmd* (−/−) ($n = 6$), Mab2256-treated *nmd* (−/− Ab) mice (upper graph, $n = 6$) and NT-4/5-treated mice (−/− NT4/5) (lower graph, $n = 3$). (**F**) Percent of depression of the CMAP amplitudes at the quasi-steady-state level for stimulation frequencies from 10 to 100 Hz. All data are from EMG recordings done at P69–71.

However, the amount of depression of the response at the end of the train was not significantly different in Mab2256-treated and untreated wild-type mice (78 ± 9%, $n = 8$ and 82.5 ± 7.4%, $n = 6$, respectively) (Fig. 3E, upper graph) ($P < 0.73$), suggesting that the treatment with the monoclonal antibody did not alter normal neuromuscular function.

In NT-4/5-treated *nmd* mice, the normalized amplitude of the final steady-state CMAP was also significantly larger at 100 Hz (79 ± 2.5%; $n = 3$) (Fig. 3D, lower trace; Fig. 3E, filled circles in lower graph) than in PBS-injected mutants ($P < 0.02$). The amount of depression at different frequencies (10, 20, 50 and 100 Hz) in wild-type, Mab2256-treated and untreated mutants are shown in Figure 3F. These results suggest that both Mab2256 and NT-4/5 were able to restore, almost completely, the normal levels of high frequency-induced neuromuscular depression.

Functional state of spindle afferent fibres in *nmd* mice

To assess the functional state of muscle spindle afferent fibres in untreated and Mab2256-treated *nmd* mice, we recorded H-waves from the dorsal foot muscles, where they are easily detectable. H-waves are elicited by the activation of motor fibres through the monosynaptic proprioceptive sensory afferent circuit (Fig. 4A, inset) and are preceded by M-waves, which are elicited by the direct stimulation of nerve motor fibres (Fig. 4A). The M/H-wave ratios were not different in wild-type (6.1 ± 1.3, $n = 6$), untreated *nmd* (6.1 ± 0.9, $n = 5$) and Mab2256-treated *nmd* mice (7.6 ± 2.6, $n = 4$), suggesting that muscle spindle fibres responsible for the stretch reflex in the dorsal foot muscles are not preferentially lost in mutants and that the treatment did not affect this circuit.

In dorsal foot muscles, we also studied the amount of depression of the EMG responses at different stimulation frequencies in *nmd* and control mice. There were no significant differences in mean quasi-steady-state depression of the CMAPs between wild-type and *nmd* mice at frequencies from 10 to 50 Hz (Fig. 4B). Only at 100 Hz (Fig. 4C), the amount of depression was slightly larger in *nmd* mice (40 ± 1.6%, $n = 6$) than in wild-type (32 ± 2.85%, $n = 6$) ($P < 0.036$), suggesting that the foot dorsal muscles are less affected than the MG in this animal model.

Motor unit number estimation analysis

The reduction in the amplitude of the CMAPs recorded in the MG of *nmd* mice suggests a decrease in the number of functional motor units. We used motor unit number estimation (MUNE) to evaluate the degree of motor neuron loss in the MG of *nmd* mice. The number of functional motor units was determined at a late period in the life of mutant mice (P215–P230), and compared with that of control littermates. At this age, muscular atrophy of the hind limbs was very severe in the mutants, whereas no signs of muscle wasting or strength decrement were observed in the heterozygous. Successive incremental stimuli produced regular increments in motor unit potentials in the controls (Fig. 5A), whereas they elicited abnormally large motor units potentials in *nmd* mice (Fig. 5B). The final size of the potential after 10 'successful' stimuli of increasing strength (i.e. stimuli that elicited an increment in the amplitude of the response) was much larger in the mutants than in the control sib mice due to the presence of large step increments in the mutants (i.e. giant motor units). Quantification of the size of the potentials is shown in the graphs in Figure 5C–F from two control (heterozygous) and two mutant littermates. The average single motor unit action potential (SMUAP) amplitude was 1.21 ± 0.62 mV ($n = 3$) in *nmd* mice and 0.178 ± 0.06 mV ($n = 3$) in control mice. Consequently, the MUNE was reduced >50% in *nmd* mice (mean value of 37.5 ± 11.4, $n = 3$) when compared with the heterozygous littermates (105.5 ± 12.4, $n = 3$, $P < 0.0015$). Moreover, low-intensity stimuli adequate for control mouse failed to elicit any response in the mutants, indicating that the threshold for fibre activation was increased in most of the remaining motor units of the mutant (data not shown). The existence of giant motor units is an indication of axonal sprouting and reinnervation of denervated muscle fibres that probably compensate, at least partially, for the severe loss in neuromuscular transmission. However, if the mutant strength depended primarily on the giant motor units, the loss of these units may lead to an abrupt failure in muscular function later on.

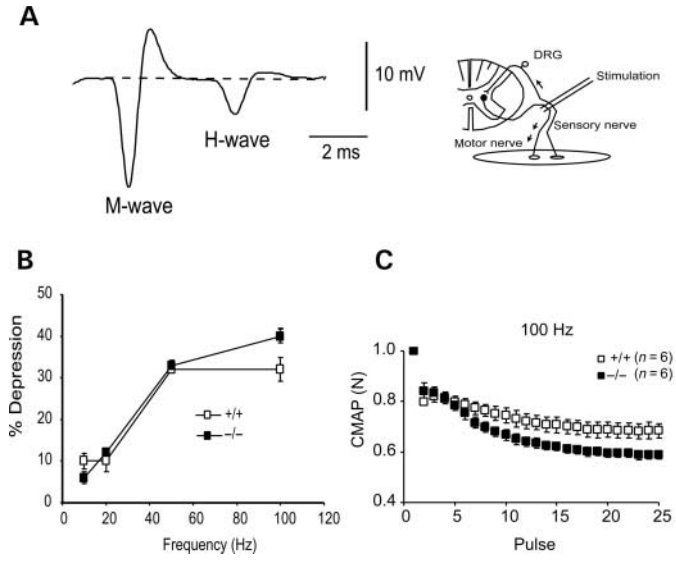

Figure 4. EMG measurements of CMAP amplitudes in the dorsal foot muscles. (**A**) M- and H-waves elicited by a single pulse stimulus in a wild-type mouse. (**B**) Percent of depression of the CMAP amplitudes at the quasi-steady-state level for stimulation frequencies from 10–100 Hz in wild-type (+/+) ($n = 6$) and *nmd* mice (−/−) ($n = 6$). (**C**) Time course of the depression of the CMAP amplitudes (normalized to the first response) during a train of stimuli of 250 ms at 100 Hz in wild-type mice ($n = 6$) and PBS injected *nmd* ($n = 6$). All data are from mice at P69–71.

Diaphragmatic function in *nmd* mice

Respiratory failure is a characteristic of human SMARD1 as early as the first year of life (4). To assess the respiratory function in *nmd* mice and the potential efficacy of the monoclonal antibody, we examine the electrophysiological property of the diaphragm of mice under anaesthetic conditions. Twelve mice older than 10 weeks were included in this study: controls

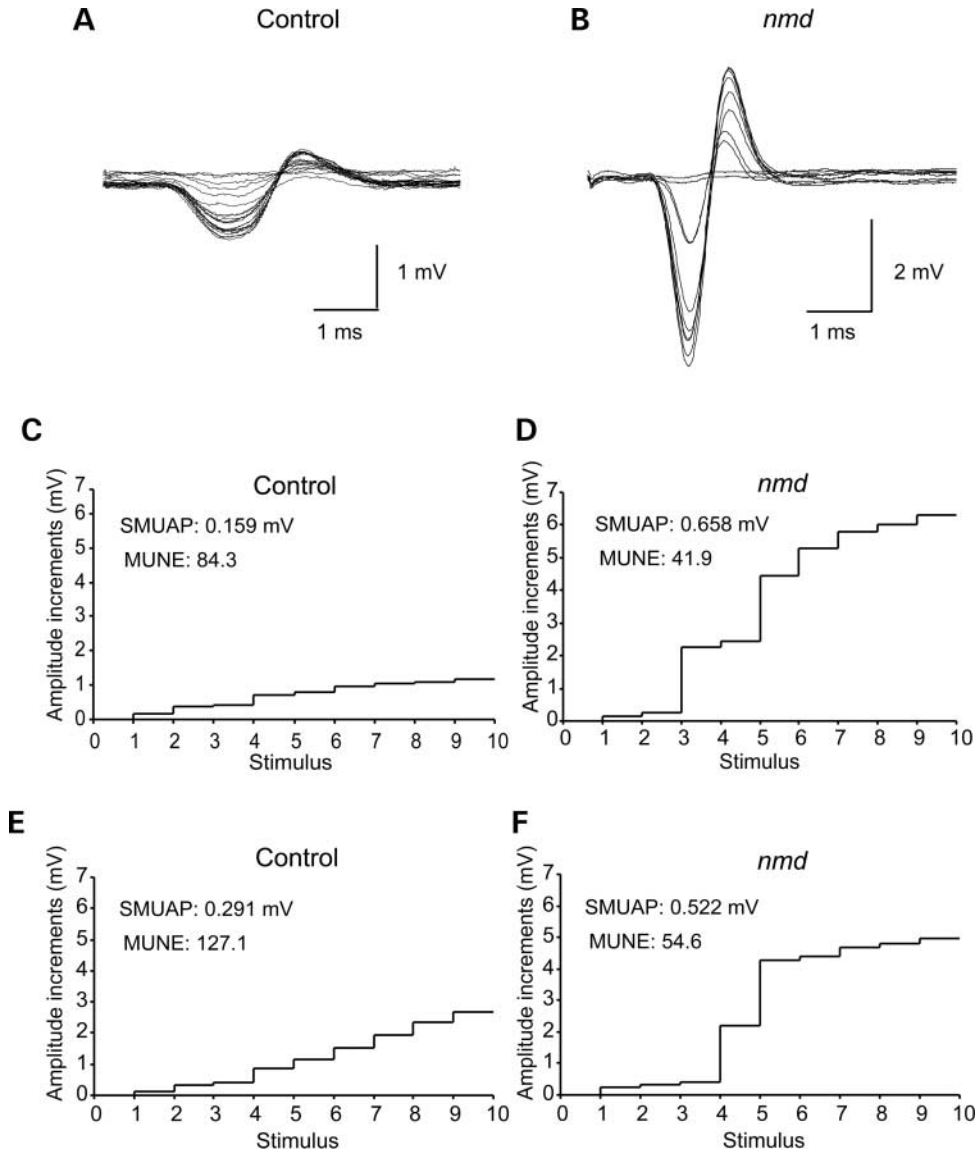

Figure 5. MUNE from the MG in mice at P215–230. (**A** and **B**) Motor unit traces from wild-type (A) and *nmd* (B) mice. (**C**–**F**) Amplitudes of SMUAPs in control (C and E) and *nmd* sib mutants (D and F) mice in response to stimuli of increasing amplitude. Each number in the *x*-axis represents a stimulus that elicited an increment in the amplitude of the response. Control animals were heterozygous.

(wild-types and heterozygous, $n = 6$), untreated *nmd* mice ($n = 3$) and Mab2256-treated *nmd* mice ($n = 3$). The electrical activity in the diaphragm is characterized by alternating bursts of spontaneous action potentials (inspiratory burst) and silent periods that coincide with expiration. Representative recordings from the diaphragm in a control and in an untreated *nmd* mouse are shown in the lower traces in Figure 6A and B. In general, no postinspiratory electrical activity was observed in control and *nmd* mice. We found that there was little variability in the duration and in the activity of the inspiratory burst (TI). The respiratory frequency in control mice (140.2 ± 15.7 bpm, $n = 6$) was similar to untreated nmd (141.7 ± 6.2 bpm, $n = 3$) and Mab2256-treated *nmd* mice (132.9 ± 22.6, $n = 3$). However, there was a significant reduction (28%) in the mean duration of the inspiration (TI) in untreated *nmd* mice (131.6 ± 4.1 ms) in comparison with control littermates (184.1 ± 11.7 ms) ($P < 0.005$), suggesting that *nmd* mice, at late stages of life, have a mild abnormal inspiratory motor discharge. In Mab2256-treated *nmd* mice, TI was 146.3 ± 8.2 ms, slightly larger than that in untreated *nmd* mice. This difference did not reach statistical significance probably owing to the small sample size ($P < 0.08$) (Fig. 6C). Histological examination of phrenic nerves' transverse sections (Fig. 6D) in very old mutants (38 weeks) showed no significant differences in the number of myelinated axons between *nmd* (337 ± 18 axons, $n = 2$) and control littermates (364 ± 11 axons, $n = 2$) (Fig. 6E). This suggests that a functional deficit, rather than an anatomical loss, of the phrenic nerves is underlying the respiratory dysfunction in *nmd* mice.

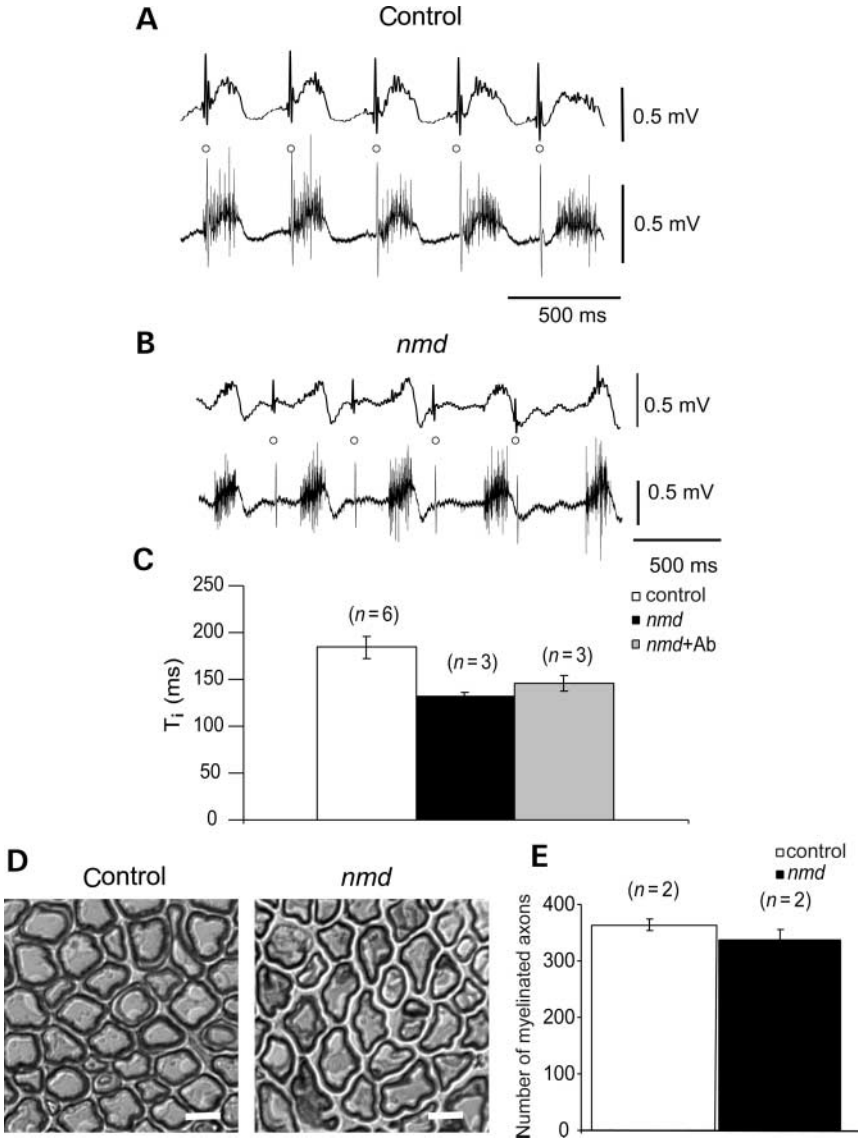

Figure 6. Spontaneous electrical activity in the diaphragm recorded *in vivo.* (**A** and **B**) Representative recordings from control (A) and *nmd* mice (B). Lower traces are raw recordings and upper traces are the integral of lower traces. Circles signal electrical activity from the heart. (**C**) Histogram showing the mean duration of the inspiration bursts (TI, in ms) in control (white bar) and PBS-injected mutant (black bar) and Mab2256-treated mutant mice (grey bar). (**D**) Histological sections of control and *nmd* phrenic nerves. **(E)** Quantification of the number of myelinated axons in four 38-week-old mice showing no significant differences between control and *nmd* littermates. Bars: 7 μm.

DISCUSSION

We have studied the electromyographic properties of the *nmd* mice and tested the efficacy of an agonistic monoclonal antibody for trkC receptors (Mab2256) on the clinical and electrophysiological progression of the disease. We show that Mab2256 treatment delayed several weeks the decline of muscular strength and it led to the electrophysiological improvement of muscular function.

Neuromuscular impairment in *nmd* mice

We observed some striking changes in *nmd* neuromuscular function. The major defects include a severe loss of motor nerve fibres and the inability of *nmd* mice to maintain a normal neuromuscular transmission with repetitive nerve stimulation. Normally, with repetitive nerve stimulation, the CMAPs gradually decline in amplitude until they reach a steady level of depression after several pulses, being the maximal degree of depression directly proportional to the stimulation frequency. We have compared this physiological response in the MG of *nmd* and wild-type and found that the *nmd* mice presented a much more severe depression in CMAP amplitudes than the littermate controls, which is consistent with their clinical weakness and it is a common finding in other mouse models of motor neuron impairment (18). It would be of interest in the future to check whether this phenomenon in *nmd* mice is due to a defect at the presynaptic

terminal, a reduction of postsynaptic efficacy or a shift of the muscular fibres to a more fatigable phenotype.

CMAP mean amplitude was reduced by >50% in *nmd* mice MG on P70. This is in agreement with the reduction to 41% of lumbar motor neurons at 5 weeks described previously in this mutant (11). At later stages of the disease (P150–230), the number of motor units remaining in the MG muscle was reduced to a 35% of the control value, which is not far from the previous estimation of 28% motor neurons remaining in the lumbar spinal cord at 12–14 weeks (11). The giant motor unit potentials had a high threshold of activation so they may recruit poorly. The severe loss of motor units, together with the inability to maintain effective transmission with repetitive stimuli, explains the diminished muscular strength of these animals.

Therapeutic potential of neurotrophic factors

Neurotrophic factors support survival of spinal motor neurons and have been shown to have a positive effect on alleviating the pathological symptoms in animal models of motor neuron diseases (14,19,20). On the basis of these results, recombinant neurotrophic factors have been considered for more than a decade as potential therapeutic drugs for motor neuron diseases. However, clinical trials had encountered problems such as inadequate dosage, side effects, etc. (21,22). Agonist monoclonal antibodies for neurotrophin receptors have several theoretical advantages over exogenous administrated neurotrophic factors, e.g. their specificity for a given trophic receptor that may reduce side effects and their long circulating half-life that facilitate the drug administration and the maintenance of therapeutic concentrations. Nevertheless, these molecules need to be studied and validated in animal models. For example, in some models the rescue of motor neurons by neurotrophic factors was found to be transient in nature (23,24). In our experiments in *nmd* mice, Mab2256 retarded but not arrested disease progression.

It has been shown that ciliary neurotrophic factor (CNTF) and NT-3 can increase life span in the mouse mutant *pmn* (progressive motor neuronopathy) (14,25,26). Average life span of *nmd* mice has been described to be 54 days (10). In our animal facility, untreated *nmd* mice median survival was similar (64 days). Treatment of *nmd* mice with Mab2256 from the third to the 11th postnatal week did not increase significantly the survival probability (median: 69 days). This result is in accordance with the fact that neuronal expression of full-length IGHMBP2 in *nmd* mice also could not improve their survival (10).

A possible explanation of the transient effects of Mab2256 is that the relative high levels of the drug in plasma reached by some animals might have produced down-regulation of trkC receptors, as has been shown in other studies with neurotrophins (27,28). If this is the case, therapeutic dosage and dosing frequency should be adjusted to avoid this effect.

Alternatively, Mab2256 was less potent (~3000-fold difference in the EC_{50}) and less effective (~3-fold difference in the maximal effect) than NT-3 in the neuronal survival bioassay. Thus, a higher affinity/activity version of the Mab2256 antibody might be required to achieve a longer and greater efficacy in the *nmd* mouse model.

Furthermore, lower motor neurons express both trkB and trkC receptors. Activation of these and perhaps other neurotrophin receptors may be necessary for clinically beneficial outcomes in the *nmd* mice. In the future, it will be important to test whether the application of both trkB and trkC agonists simultaneously would provide greater therapeutic benefits in this disease model. Indeed, we found that both Mab2256 and NT-4/5, an endogenous trkB agonist, can restore aspects of the electrophysiological properties of the neuromuscular junction (NMJ), such as in the repeated stimulation protocol, of the *nmd* mice. Combination of NT-3 with other neurotrophic factors may be also suitable; for example, co-injection of adenovirus vectors encoding the *CNTF* gene and the *NT-3* gene into skeletal muscle cells of *pmn* mice produces a large increase in axonal survival than either vector alone (26,29).

We do not yet know the exact cellular target(s) responsible for the positive effects seen *in vivo* with Mab2256 in *nmd* mice, but they may be motor neurons, muscle cells, glia cells or a combination of these. Motor neurons express the NT-3 receptor trkC and respond to NT-3 with increasing survival (15,30–32). Recent evidences suggest that NT-3, besides its effect on the survival of motor neurons, may influence the efficacy of neuromuscular transmission (33–36). Exogenous brain-derived neurotrophic factor (BDNF) or NT-3 (but not nerve growth factor, NGF) potentiate both spontaneous and impulse-evoked synaptic activity of developing neuromuscular synapses in culture, an effect that seems to be mediated by the trkC receptor and persists as long as the factor is present (37). Furthermore, treatment of isolated neurons with NT-3 for 2 days increases the average sizes of quantal ACh packets at newly formed nerve-muscle synapses, whereas treatment with antibody against NT-3 or with K252a, a specific inhibitor of tyrosine kinase receptors, decreases the quantal size at existing synapses, which suggests that NT-3 may be responsible for the development and maintenance of the quantal packets (34). Enhancement of synaptic transmission by NT-3 has also been reported in adult hippocampus slices (38). NT-3 and NT-4/5 synthesized by the muscle may act in a retrograde manner on presynaptic motor neurons, thereby affecting the continued functional differentiation of the neurons by, for example, increasing the synthesis of ACh and neuregulin (39). Besides these presynaptic effects, muscle-secreted neurotrophins (BDNF, NT-3, NT-4/5 and GDNF) (15,40–43) may act on the muscle fibres themselves in an autocrine manner. Exogenous administration of NT-3 has been shown to restore NMJ architecture in curare-treated muscles previously altered by the treatment (44). The release of NT-3 from muscle cells seems to be regulated, in turn, by the synaptic activity at the NMJ (36).

Adenovirus-mediated gene transfer of *NT-3* promotes terminal sprouting of motor fibres in *pmn* mice, which suggests that NT-3 is also involved in the maintenance and regeneration of distal axon structures (26,29). Additionally, neurotrophic factors may also influence the axonal transport from the motor nerves to the spinal cord. In the *pmn* mice, in which motor axons degenerate due to altered tubulin assembly (45), retrograde transport of fluorescent tracers either injected into the gastrocnemius muscle or applied directly onto the cut sciatic nerve can be improved by CNTF, BDNF or NT-3, but not by GDNF or NGF (46).

It is unlikely that Mab2256 can cross the intact brain–blood barrier due to its large molecular size; however, NT-3, and other neurotrophins (NT-4/5, BDNF) can be retrogradely transported along the motor neuron axons to their somata (31,42,47,48). It would be of great interest to know whether this monoclonal antibody, once bound to trkC, could be transported retrogradely and have a direct effect on the cell body of motor neurons. The exact site(s) of action of the trkC antibody and its mode of action clearly await for further investigation.

Diaphragm electrical activity

In SMARD1 patients, paralysis of the diaphragm appears during the first 13 months of life (2), but in the *nmd* mice, breathing abnormalities manifested relatively late (10). To evaluate the functional state of the diaphragm during the final stages of the disease (P150–230), we recorded the spontaneous electrical activity of the diaphragm of mutant mice *in vivo*. In anaesthetized mice, no difference in the mean respiratory frequency was found between control and mutant littermates, but we discovered a 26% reduction in the duration of the inspiration (TI), with a concomitant decrease in the number of action potentials during each inspiratory burst, which may produce a certain reduction in diaphragm strength. From our recordings, we cannot discern whether there are non-functioning regions within the diaphragm, as it was difficult to distinguish between zones with no-electrical-activity and mispositioning of the active electrode (see Materials and Methods). The presence of abundant myopathic changes in the diaphragm of *nmd* mice has been recently described (11). In addition, these mice also suffer from congestive heart failure and a muscle dystrophy-like phenotype (10), which may secondarily contribute to the respiratory distress. The number of myelinated axons, however, was not reduced in the very old *nmd* mice (38 weeks), which is in accordance with what it has been found in 14-week-old *nmd* mice (11), and in agreement with the expression of a certain amount of full-length functional IGHMBP2 protein (9).

In conclusion, we have found that Mab2256 treatment on *nmd* mice produced a significant but transient improvement of muscular strength, as well as normalization of the amount of neuromuscular depression during high-frequency nerve stimulation. Further study to elucidate the mechanism of action of this effect, together with a more complete characterization of presynaptic and postsynaptic events during neurotransmission at the NMJ should help us understand the neuromuscular defect in *nmd* mice, the physiological role of IGHMBP2 in motor neurons and search for the rational therapeutic approach of this terrible disease.

MATERIALS AND METHODS

Mice breeding and genotype

B6.BLKS-*nmd*^{2J} mice were obtained from The Jackson Laboratory. Mice heterozygous for the *nmd*^{2J} were intercrossed and wild-type, heterozygous and mutant mice were used for the experiments. Mice were bred and maintained in standard conditions, except that for mutants, food and water were available at the floor cage level.

Mice were genotyped as described (9). Briefly, the point mutation, cause of the phenotype of the *nmd* mouse (homozygous for this mutation), generates a new *Dde* I restriction site that is absent in wild-type mice. The PCR assay to identify carriers in unaffected offspring was performed with two oligonucleotide primers, which amplify a 694 bp PCR product, where the mutation is, being the forward primer: 5′-GCTGGAAACGATCACATACCG-3′ and the reverse primer: 5′-AGCTCCTGATGATCCAATGG-3′.

Mice treatment

Random groups of coded littermates mice of both sexes were injected intraperitoneally either with the monoclonal antibody Mab2256 (5 mg/kg body weight, two times per week, from 20–21 days of age; Rinat Neuroscience, Palo Alto, CA, USA), human recombinant NT-4/5 (5 mg/kg body weight, two times per week, from 21 days of age; Genentech, San Francisco, CA, USA) or PBS. All animal manipulations were performed in accordance with institutional guidelines and permissions.

Receptor tyrosine phosphorylation assay

The agonist activity of Mab2256 was evaluated in a cell-based trkC receptor tyrosine phosphorylation assay as previously described (16). The half maximum effective concentrations were estimated by non-linear curve fitting using the Prism Software (GraphPad, San Diego, CA, USA).

Embryonic trigeminal neuron survival assay

Dissociated cultures of the trigeminal neurons were established from E12 Sprague–Dawley rats. Dissected ganglia were trypsinized and dissociated by trituration (49). The neurons were plated at a low density in 96-well tissue culture plates in a defined, serum-free medium on a polyornithine/laminin substratum. NT-3 and the Mab2256 antibody, at varying concentrations, were added to the cultures at the time of plating in triplicates and in quadruplicates, respectively. To quantify neuronal survival under each of the different conditions, the numbers of the neurons that survived at 48 h after plating were counted. The half maximum effective concentrations were estimated by non-linear curve fitting using the Prism Software (GraphPad).

Pharmacokinetic study

Adult female CD-1 mice ($n = 3$) were injected intraperitoneally with Mab2256 at 2 mg/kg. The animals were then bled subsequently at 24, 48, 136 and 184 h postinjection. The serum concentration of Mab2256 at different time points were determined as described subsequently.

Determination of monoclonal antibody concentrations

The serum level of mouse monoclonal antibody Mab2256 was determined by a standard sandwich ELISA. The 96-well

Maxisorp plate (Nunc) was preabsorbed overnight at 4°C with 0.2 mg/ml of a protein A column-purified, recombinant human trkC extracellular domain–IgG Fc fusion protein (Rinat Neuroscience) expressed by transient transfection of HEK293 cells. The trkC-coated plate was then blocked at 25°C for 1 h with PBS with 0.5% bovine serum albumin and 0.05% Tween-20. The plate was washed three times in PBS with 0.05% Tween-20. The standard dilution series of Mab2256 as well as appropriately diluted serum samples were incubated in the plate at 25°C for 1 h, followed by three washes. The horseradish peroxidase (HRP)-conjugated rabbit anti-mouse IgG (Jackson ImmunoResearch) was applied at 1:5000, incubated at 25°C for 1 h to detect the bound mouse monoclonal antibody. Finally, the signals were detected by the colorimetric reaction of HRP with TMB substrate (KPL, Denmark).

Neurological tests

Mutant and littermate control mice were subjected to standard neurological examination to quantify the onset and extension of the neuromuscular defect (SHIRPA protocol; http://www.mgu.har.mrc.ac.uk/mutabase/shirpa_summary.html) (50). For balance measurements, mice were lowered onto a square thin stick by tail suspension and allowed to stand on top. The stick was then rotated each second by hand for 10 s and the ability of the mice to remain on the stick was measured in seconds.

For fore limb grip strength, mice were held above a horizontal wire and lowered to allow the fore limbs to grip the wire The ability of the mice to remain attached by the fore limbs was scored during 10 s.

Electromyography

Intramuscular compound action potentials (CMAP) were recorded as previously described (18) from anaesthetized (100 mg/kg ketamine + 10 mg/kg xylazine) wild-type and *nmd* mice at P70. Briefly, recording needle electrodes were placed either into the dorsal foot muscles with a reference electrode at the base of the fifth phalanx or into the medial part of the gastrocnemius (MG). A ground electrode was placed at the base of the tail. Stimulating needle electrodes were placed at the sciatic notch and the head of the fibula. Stimulation protocols of supramaximal current pulses (0.05 ms duration, 5 mA amplitude) were applied either as single pulses or as short duration train of pulses of 10, 20, 50 and 100 Hz. Stimulation pulses were generated by an isolated pulse stimulator (A-M Systems, Model 2100). Recorded outputs were differentially amplified (Brownlee Precision, Model 210A), digitally acquired at 20 000 samples/s (ADInstruments, PowerLab/4SP) and stored in a computer for later analysis.

MUNE from the MG was calculated by dividing the averaged size of a single motor unit potential into a maximal CMAP, which represents the sum of all motor units. Sampling of single motor unit potentials was done by the incremental method (51,52) that consists in the application of finely controlled current in very small steps from subthreshold levels until the progressive recruitment of 10 responses. Each current amplitude was applied three times and was considered stable, and therefore accepted, if they were identical. Individual motor unit amplitudes were obtained by subtracting amplitudes to each response from that of the previous response. The average of the individual values gave us an estimation of the SMUAP size.

In vivo diaphragmatic recordings were performed by inserting a needle electrode behind the xyphoid process slightly off the middle line to either side. The reference electrode was placed on the chest and the ground electrode at the base of the tail. The diaphragm was readily identified by rhythmical burst discharges synchronous with respiration. The inspiratory discharges were quantified by the peak amplitude and area of the integral of the recording. Inspiratory durations (TI) were also analysed. Averaged values were calculated from six consecutive breathing cycles.

Studies were performed with coded mice so that the electromyographer was blinded as to which mice were being tested.

All data are reported as mean ± SEM. Statistical significance was evaluated using a Student's *t*-test. The criterion level for determination of statistical significance was set at $P < 0.05$ for all experiments.

Histology

Mice were sacrificed with an overdose of ketamine/xylazine and right side phrenic nerves were obtained close to their entry into the diaphragm muscle. Nerves were fixed with 4% paraformaldehyde and 2.5% glutaraldehyde fixative in PBS, and then postfixed with 2% osmium tetroxide and embedded in spurr resine (plastic embedding). Sections of 2 μm thick were stained with Toluidine blue and examined by light microscopy (Axiovert 35, Zeiss). Myelinated axons were counted for each nerve.

ACKNOWLEDGEMENTS

We are grateful to Drs Michael Sendtner, Guillermo Alvarez de Toledo and Rafael Fernandez-Chacón for helpful comments and Drs José Luis Villar and Enrique Ráfel Ribas for nerve histology processing. Thanks to Itziar Benito for help on animal injections; Jörg Zeller for antibody purification. This work was supported by grants from MEC BFI2004-00350 and BFI2001-3199 to L.T. R.R. was supported by a fellowship from Rinat Neuroscience.

Conflict of Interest statement. None declared.

REFERENCES

1. Lefebvre, S., Burglen, L., Reboullet, S., Clermont, O., Burlet, P., Viollet, L., Benichou, B., Cruaud, C., Millasseau, P., Zeviani, M. *et al.* (1995) Identification and characterization of a spinal muscular atrophy-determining gene. *Cell*, **80**, 155–165.
2. Grohmann, K., Wienker, T.F., Saar, K., Rudnik-Schoneborn, S., Stoltenburg-Didinger, G., Rossi, R., Novelli, G., Nurnberg, G., Pfeufer, A., Wirth, B. *et al.* (1999) Diaphragmatic spinal muscular atrophy with respiratory distress is heterogeneous, and one form is linked to chromosome 11q13–q21. *Am. J. Hum. Genet.*, **65**, 1459–1462.

3. Grohmann, K., Schuelke, M., Diers, A., Hoffmann, K., Lucke, B., Adams, C., Bertini, E., Leonhardt-Horti, H., Muntoni, F., Ouvrier, R. *et al.* (2001) Mutations in the gene encoding immunoglobulin mu-binding protein 2 cause spinal muscular atrophy with respiratory distress type 1. *Nat. Genet.*, **29**, 75–77.
4. Grohmann, K., Varon, R., Stolz, P., Schuelke, M., Janetzki, C., Bertini, E., Bushby, K., Muntoni, F., Ouvrier, R., van Maldergem, L. *et al.* (2003) Infantile spinal muscular atrophy with respiratory distress type 1 (SMARD1). *Ann. Neurol.*, **54**, 719–724.
5. Pitt, M., Houlden, H., Jacobs, J., Mok, Q., Harding, B., Reilly, M. and Surtees, R. (2003) Severe infantile neuropathy with diaphragmatic weakness and its relationship to SMARD1. *Brain*, **126**, 2682–2692.
6. Wirth, B. (2000) An update of the mutation spectrum of the survival motor neuron gene (SMN1) in autosomal recessive spinal muscular atrophy (SMA). *Hum. Mutat.*, **15**, 228–237.
7. Mercuri, E., Bertini, E., Messina, S., Pelliccioni, M., D'Amico, A., Colitto, F., Mirabella, M., Tiziano, F.D., Vitali, T., Angelozzi, C. *et al.* (2004) Pilot trial of phenylbutyrate in spinal muscular atrophy. *Neuromuscul. Disord.*, **14**, 130–135.
8. Cook, S.A., Johnson, K.R., Bronson, R.T. and Davisson, M.T. (1995) Neuromuscular degeneration (nmd): a mutation on mouse chromosome 19 that causes motor neuron degeneration. *Mamm. Genome*, **6**, 187–191.
9. Cox, G.A., Mahaffey, C.L. and Frankel, W.N. (1998) Identification of the mouse neuromuscular degeneration gene and mapping of a second site suppressor allele. *Neuron*, **21**, 1327–1337.
10. Maddatu, T.P., Garvey, S.M., Schroeder, D.G., Hampton, T.G. and Cox, G.A. (2004) Transgenic rescue of neurogenic atrophy in the nmd mouse reveals a role for Ighmbp2 in dilated cardiomyopathy. *Hum. Mol. Genet.*, **13**, 1105–1115.
11. Grohmann, K., Rossoll, W., Kobsar, I., Holtmann, B., Jablonka, S., Wessig, C., Stoltenburg-Didinger, G., Fischer, U., Hubner, C., Martini, R. *et al.* (2004) Characterization of Ighmbp2 in motor neurons and implications for the pathomechanism in a mouse model of human spinal muscular atrophy with respiratory distress type 1 (SMARD1). *Hum. Mol. Genet.*, **13**, 2031–2042.
12. Arakawa, Y., Sendtner, M. and Thoenen, H. (1990) Survival effect of ciliary neurotrophic factor (CNTF) on chick embryonic motoneurons in culture: comparison with other neurotrophic factors and cytokines. *J. Neurosci.*, **10**, 3507–3515.
13. Sendtner, M., Kreutzberg, G.W. and Thoenen, H. (1990) Ciliary neurotrophic factor prevents the degeneration of motor neurons after axotomy. *Nature*, **345**, 440–441.
14. Sendtner, M., Schmalbruch, H., Stockli, K.A., Carroll, P., Kreutzberg, G.W. and Thoenen, H. (1992) Ciliary neurotrophic factor prevents degeneration of motor neurons in mouse mutant progressive motor neuronopathy. *Nature*, **358**, 502–524.
15. Henderson, C.E., Camu, W., Mettling, C., Gouin, A., Poulsen, K., Karihaloo, M., Rullamas, J., Evans, T., McMahon, S.B., Armanini, M.P. *et al.* (1993) Neurotrophins promote motor neuron survival and are present in embryonic limb bud. *Nature*, **363**, 266–270.
16. Sadick, M.D., Galloway, A., Shelton, D., Hale, V., Weck, S., Anicetti, V. and Wong, W.L. (1997) Analysis of neurotrophin/receptor interactions with a gD-flag-modified quantitative kinase receptor activation (gD.KIRA) enzyme-linked immunosorbent assay. *Exp. Cell Res.*, **234**, 354–361.
17. Poduslo, J.F. and Curran, G.L. (1996) Permeability at the blood–brain and blood–nerve barriers of the neurotrophic factors: NGF, CNTF, NT-3, BDNF. *Brain Res. Mol. Brain Res.*, **36**, 280–286.
18. Fernandez-Chacon, R., Wolfel, M., Nishimune, H., Tabares, L., Schmitz, F., Castellano-Munoz, M., Rosenmund, C., Montesinos, M.L., Sanes, J.R., Schneggenburger, R. *et al.* (2004) The synaptic vesicle protein CSP alpha prevents presynaptic degeneration. *Neuron*, **42**, 237–251.
19. Sagot, Y., Vejsada, R. and Kato, A.C. (1997) Clinical and molecular aspects of motoneurone diseases: animal models, neurotrophic factors and Bcl-2 oncoprotein. *Trends Pharmacol. Sci.*, **18**, 330–337.
20. Mitsumoto, H., Ikeda, K., Klinkosz, B., Cedarbaum, J.M., Wong, V. and Lindsay, R.M. (1994) Arrest of motor neuron disease in wobbler mice cotreated with CNTF and BDNF. *Science*, **265**, 1107–1110.
21. Miller, R.G., Petajan, J.H., Bryan, W.W., Armon, C., Barohn, R.J., Goodpasture, J.C., Hoagland, R.J., Parry, G.J., Ross, M.A. and Stromatt, S.C. (1996) A placebo-controlled trial of recombinant human ciliary neurotrophic (rhCNTF) factor in amyotrophic lateral sclerosis. rhCNTF ALS Study Group. *Ann. Neurol.*, **39**, 256–260.
22. Thoenen, H. and Sendtner, M. (2002) Neurotrophins: from enthusiastic expectations through sobering experiences to rational therapeutic approaches. *Nat. Neurosci.*, **5 (**suppl.), 1046–1050.
23. Diener, P.S. and Bregman, B.S. (1994) Neurotrophic factors prevent the death of CNS neurons after spinal cord lesions in newborn rats. *Neuroreport*, **5**, 1913–1917.
24. Vejsada, R., Sagot, Y. and Kato, A.C. (1995) Quantitative comparison of the transient rescue effects of neurotrophic factors on axotomized motoneurons *in vivo. Eur. J. Neurosci.*, **7**, 108–115.
25. Sagot, Y., Tan, S.A., Baetge, E., Schmalbruch, H., Kato, A.C. and Aebischer, P. (1995) Polymer encapsulated cell lines genetically engineered to release ciliary neurotrophic factor can slow down progressive motor neuronopathy in the mouse. *Eur. J. Neurosci.*, **7**, 1313–1322.
26. Haase, G., Kennel, P., Pettmann, B., Vigne, E., Akli, S., Revah, F., Schmalbruch, H. and Kahn, A. (1997) Gene therapy of murine motor neuron disease using adenoviral vectors for neurotrophic factors. *Nat. Med.*, **3**, 429–436.
27. Bibel, M. and Barde, Y.A. (2000) Neurotrophins: key regulators of cell fate and cell shape in the vertebrate nervous system. *Genes Dev.*, **14**, 2919–2937.
28. Knusel, B., Gao, H., Okazaki, T., Yoshida, T., Mori, N., Hefti, F. and Kaplan, D.R. (1997) Ligand-induced down-regulation of Trk messenger RNA, protein and tyrosine phosphorylation in rat cortical neurons. *Neuroscience*, **78**, 851–862.
29. Sendtner, M. (1997) Gene therapy for motor neuron disease. *Nat. Med.*, **3**, 380–381.
30. Oppenheim, R.W. (1996) Neurotrophic survival molecules for motoneurons: an embarrassment of riches. *Neuron*, **17**, 195–197.
31. Yan, Q., Elliott, J.L., Matheson, C., Sun, J., Zhang, L., Mu, X., Rex, K.L. and Snider, W.D. (1993) Influences of neurotrophins on mammalian motoneurons *in vivo. J. Neurobiol.*, **24**, 1555–1577.
32. Duberley, R.M., Johnson, I.P., Anand, P., Leigh, P.N. and Cairns, N.J. (1997) Neurotrophin-3-like immunoreactivity and Trk C expression in human spinal motoneurones in amyotrophic lateral sclerosis. *J. Neurol. Sci.*, **148**, 33–40.
33. Wang, T., Xie, K. and Lu, B. (1995) Neurotrophins promote maturation of developing neuromuscular synapses. *J. Neurosci.*, **15**, 4796–4805.
34. Liou, J.C. and Fu, W.M. (1997) Regulation of quantal secretion from developing motoneurons by postsynaptic activity-dependent release of NT-3. *J. Neurosci.*, **17**, 2459–2468.
35. Sendtner, M. (1998) Neurotrophic factors: effects in modulating properties of the neuromuscular endplate. *Cytokine Growth Factor Rev.*, **9**, 1–7.
36. Poo, M.M. (2001) Neurotrophins as synaptic modulators. *Nat. Rev. Neurosci.*, **2**, 24–32.
37. Lohof, A.M., Ip, N.Y. and Poo, M.M. (1993) Potentiation of developing neuromuscular synapses by the neurotrophins NT-3 and BDNF. *Nature*, **363**, 350–353.
38. Kang, H. and Schuman, E.M. (1995) Long-lasting neurotrophin-induced enhancement of synaptic transmission in the adult hippocampus. *Science*, **267**, 1658–1662.
39. Loeb, J.A. and Fischbach, G.D. (1997) Neurotrophic factors increase neuregulin expression in embryonic ventral spinal cord neurons. *J. Neurosci.*, **17**, 1416–1424.
40. Griesbeck, O., Parsadanian, A.S., Sendtner, M. and Thoenen, H. (1995) Expression of neurotrophins in skeletal muscle: quantitative comparison and significance for motoneuron survival and maintenance of function. *J. Neurosci. Res.*, **42**, 21–33.
41. Henderson, C.E., Phillips, H.S., Pollock, R.A., Davies, A.M., Lemeulle, C., Armanini, M., Simmons, L., Moffet, B., Vandlen, R.A., Simpson, L.C. *et al.* (1994) GDNF: a potent survival factor for motoneurons present in peripheral nerve and muscle. *Science*, **266**, 1062–1064.
42. Koliatsos, V.E., Clatterbuck, R.E., Winslow, J.W., Cayouette, M.H. and Price, D.L. (1993) Evidence that brain-derived neurotrophic factor is a trophic factor for motor neurons *in vivo. Neuron*, **10**, 359–367.
43. Funakoshi, H., Frisen, J., Barbany, G., Timmusk, T., Zachrisson, O., Verge, V.M. and Persson, H. (1993) Differential expression of mRNAs for neurotrophins and their receptors after axotomy of the sciatic nerve. *J. Cell Biol.*, **123**, 455–465.

44. Loeb, J.A., Hmadcha, A., Fischbach, G.D., Land, S.J. and Zakarian, V.L. (2002) Neuregulin expression at neuromuscular synapses is modulated by synaptic activity and neurotrophic factors. *J. Neurosci.*, **22**, 2206–2214.
45. Bommel, H., Xie, G., Rossoll, W., Wiese, S., Jablonka, S., Boehm, T. and Sendtner, M. (2002) Missense mutation in the tubulin-specific chaperone E (*Tbce*) gene in the mouse mutant progressive motor neuronopathy, a model of human motoneuron disease. *J. Cell Biol.*, **159**, 563–569.
46. Sagot, Y., Rosse, T., Vejsada, R., Perrelet, D. and Kato, A.C. (1998) Differential effects of neurotrophic factors on motoneuron retrograde labeling in a murine model of motoneuron disease. *J. Neurosci.*, **18**, 1132–1141.
47. DiStefano, P.S., Friedman, B., Radziejewski, C., Alexander, C., Boland, P., Schick, C.M., Lindsay, R.M. and Wiegand, S.J. (1992) The neurotrophins BDNF, NT-3, and NGF display distinct patterns of retrograde axonal transport in peripheral and central neurons. *Neuron*, **8**, 983–993.
48. Yan, Q., Elliott, J. and Snider, W.D. (1992) Brain-derived neurotrophic factor rescues spinal motor neurons from axotomy-induced cell death. *Nature*, **360**, 753–755.
49. Davies, A.M., Horton, A., Burton, L.E., Schmelzer, C., Vandlen, R. and Rosenthal, A. (1993) Neurotrophin-4/5 is a mammalian-specific survival factor for distinct populations of sensory neurons. *J. Neurosci.*, **13**, 4961–4967.
50. Rogers, S.D., Demaster, E., Catton, M., Ghilardi, J.R., Levin, L.A., Maggio, J.E. and Mantyh, P.W. (1997) Expression of endothelin-B receptors by glia *in vivo* is increased after CNS injury in rats, rabbits, and humans. *Exp. Neurol.*, **145**, 180–195.
51. McComas, A.J. (1991) Motor unit estimation: methods, results, and present status. *Muscle Nerve*, **14**, 585–597.
52. Shefner, J.M. and Gooch, C.L. (2002) Motor unit number estimation in neurologic disease. *Adv. Neurol.*, **88**, 33–52.